

An exact study of charge-spin separation, pairing fluctuations and pseudogaps in four-site Hubbard clusters

Armen N. Kocharian*

*Department of Physics and Astronomy,
California State University, Northridge,
CA 91330-8268*

Gayanath W. Fernando†

*Department of Physics, University of Connecticut,
Storrs, CT 06269 and IFS, Hantana Rd., Kandy, Sri Lanka*

Kalum Palandage

*Department of Physics, University of Connecticut,
Storrs, CT 06269*

James W. Davenport

*Computational Science Center,
Brookhaven National Laboratory,
Upton, NY 11973*

An exact study of charge-spin separation, pairing fluctuations and pseudogaps is carried out by combining the *analytical* eigenvalues of the four-site Hubbard clusters with the grand canonical and canonical ensemble approaches in a multidimensional parameter space of temperature (T), magnetic field (h), on-site interaction (U) and chemical potential (μ). Our results, near the average number of electrons $\langle N \rangle \approx 3$, strongly suggest the existence of a critical parameter $U_c(T)$ for the localization of electrons and a particle-hole binding (*positive*) gap $\Delta^{e-h}(T) > 0$ at $U > U_c(T)$, with a zero temperature quantum critical point, $U_c(0) = 4.584$. For $U < U_c(T)$, particle-particle pair binding is found with a (*positive*) pairing gap $\Delta^P(T) > 0$. The ground state degeneracy is lifted at $U > U_c(T)$ and the cluster becomes a Mott-Hubbard like insulator due to the presence of energy gaps at all (allowed) integer numbers ($1 \leq N \leq 8$) of electrons. In contrast, for $U \leq U_c(T)$, we find an electron pair binding instability at finite temperature near $\langle N \rangle \approx 3$, which manifests a possible pairing mechanism, a precursor to superconductivity in small clusters. Rigorous criteria for the existence of many-body Mott-Hubbard like particle-hole and particle-particle pairings, spin-spin pairing, (spin) pseudogap and (spin) antiferromagnetic critical crossover temperatures, at which the corresponding pseudogaps disappear, are also formulated. In particular, the resulting phase diagram consisting of charge and spin pseudogaps, antiferromagnetic correlations, hole pairing with competing hole-rich ($\langle N \rangle = 2$), hole-poor ($\langle N \rangle = 4$) and magnetic ($\langle N \rangle = 3$) regions in the ensemble of clusters near 1/8 filling closely resembles the phase diagrams and inhomogeneous phase separation recently found in the family of doped high T_c cuprates.

PACS numbers: 65.80.+n, 73.22.-f, 71.10.Fd, 71.27.+a, 71.30.+h, 74.20.Mn

I. INTRODUCTION

Understanding the effects of electron correlation and pseudogap phenomena [1, 2, 3, 4, 5, 6] in doped oxides, including the cuprate superconductors is one of the most challenging problems in condensed matter physics [7]. Although the experimental determination of various inhomogeneous phases in cuprates is still somewhat controversial [8], the underdoped high T_c superconductors (HTSCs) are often characterized by crossover temperatures below which excitation pseudogaps in the normal-state are seen to develop [9]. In these materials, the

spectral weight begins to be strongly suppressed below some characteristic temperature T_s that is higher than the superconducting crossover temperature T_c . There are many experiments supporting a highly nonuniform hole distribution leading to the formation of hole-rich and hole-poor regions in doped $\text{La}_{2-x}\text{Sr}_x\text{CuO}_4$ and other cuprate HTSCs [10]. This electronic phase separation is expected to be mostly pronounced at low hole concentrations. Recently, strong experimental evidence has been found for ‘electronic phase separation’ in La-cuprates near optimal doping into separate, magnetic and superconducting phases [11].

The relevance of the Hubbard model for studies of the HTSCs has been the focus of intensive research and debated for quite some time with no firm conclusions up to now. Even though the small Hubbard clusters do not have the full capacity to describe the complexity of

*Electronic address: armen.n.kocharian@csun.edu

†Electronic address: fernando@phys.uconn.edu

copper ions and their ancillary oxygens detected in the HTSC materials, it is still argued that this model can capture the essential physics of the HTSCs [1]. However, beyond one and infinite dimensions, there is no exact solution currently available for the Hubbard Hamiltonian. It is also known that in the optimally doped cuprates, the correlation length of dynamical spin fluctuations is very small [12], which points to the local character of electron interactions in the cuprates. Therefore, exact microscopic studies of pairing, crossover and pseudogaps, by using analytical diagonalization of small Hubbard clusters, which account accurately for short-range dynamical correlations, are relevant and useful with regard to understanding the physics of the HTSCs. Our exact analytical solution appears to be providing useful insight into the physical origin of the high energy insulator-metal and low energy antiferromagnetic crossovers, electron pairing and spin density fluctuations in the superconducting phase.

The following questions are central to our study: (i) When treated exactly, what essential features can the simple Hubbard clusters capture, that are in common with the HTSCs? (ii) Using simple cluster studies, is it possible to obtain a mesoscopic understanding of electron-hole/electron-electron pairing and identify various possible phases and crossover temperatures? (iii) Do these small clusters (coupled to a particle bath) contain important features that are similar to large clusters and thermodynamical systems?

Our work has uncovered important answers to the questions raised above. This is a follow-up to our recent study, in which rigorous criteria were found for the existence of microscopic quantum critical points (QCP), Mott-Hubbard (MH) and Néel type bifurcations, and corresponding critical temperatures of crossovers and various phases in finite-size systems [13]. Small 2- and 4-site clusters with short range electronic correlations provide (unique) insight into the thermodynamics and exact many body physics, difficult to obtain from approximate methods. In particular, we show that these small Hubbard clusters, in the absence of long range order, exhibit particle-particle, Mott-Hubbard like particle-hole or antiferromagnetic-paramagnetic instabilities in the ground state and at finite temperatures.

In addition, the 4-site (square) cluster is the basic building block of the CuO_2 planes in the HTSCs and it can be used as a block reference to build up larger superblocs in 2D of desirable sizes by applying Cluster Perturbation Theory (CPT) [14], non-perturbative Real-Space Renormalization Group (RSRG) [15], Contractor Renormalization Group (CORE) [16], or Dynamical Cluster Approximation (DCA) for embedded 4-site clusters coupled to an uncorrelated bath [17]. Similar attempts at studying small clusters (such as the ground state studies of weakly coupled Hubbard dimers and squares by Tsai and Kivelson [18]) have begun recently and the lessons learned here will be invaluable to such studies and useful to the condensed matter community in general. Above all, these small clusters can be synthe-

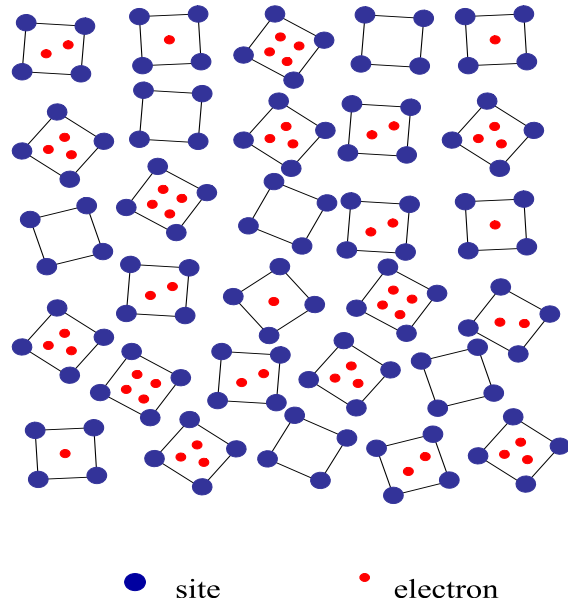


FIG. 1: Various possible configuration mixing of electrons (below half filling) that can be found in an ensemble of 4-site clusters. Note that the mixing of configurations is brought about by the temperature.

sized and utilized for understanding essential many-body physics at the mesoscopic level and hence are useful in their own right.

II. MODEL AND METHODOLOGY

The single orbital 4-site minimal Hubbard Hamiltonian,

$$H = -t \sum_{i\sigma} (c_{i\sigma}^\dagger c_{i+1\sigma} + H.c.) + U \sum_i n_{i\uparrow} n_{i\downarrow} - h \sum_i S_i^z, \quad (1)$$

with hopping t and on-site interaction U is the focus of this work. Periodic boundary conditions are used for the clusters. Unless otherwise stated, all the energies reported here are measured in units of t (i.e. t has been set to 1 in most of the equations that follow). Our calculations are based on the exact *analytical* expressions for the eigenvalue E_n of the n^{th} many-body eigenstate of the 4-site Hubbard clusters [19]. As we show here, this model, used in conjunction with the grand canonical and canonical ensembles, yields valuable insight into the physics of strongly correlated electrons.

A. Thermodynamics and response functions

The complete phase diagram of interacting electrons can be obtained with high accuracy due to the analytically (exact) given thermodynamic expressions. In

Fig. 1, possible electron configurations (below half-filling) in the grand canonical ensemble for the 4-site clusters are shown. The grand partition function Z_U (where the number of particles N and the projection of spin s^z are allowed to fluctuate) and its derivatives are calculated (exactly) without taking the thermodynamic limit. The exact grand canonical potential Ω_U for many-body interacting electrons is

$$\Omega_U = -T \ln \sum_{n \leq N_H} e^{-\frac{E_n - \mu N_n - h s_n^z}{T}}, \quad (2)$$

where N_n and s_n^z are the number of particles and the projection of spin in the n^{th} state respectively. The Hilbert space dimension in (2) is $N_H = 4^4$. The derivatives we study may be labeled as first order (such as the average spin projection/magnetization in response to an applied magnetic field) or second order (such as fluctuations/susceptibilities). These responses, evaluated as functions of chemical potential μ , applied field h , on-site Coulomb interaction U and temperature T , carry a wealth of information that can be used to identify various phases and phase boundaries. Some of these results for the 2- and 4-site clusters were reported earlier [13].

The (first order) responses due to doping and external magnetic field are as follows:

$$\langle N \rangle = -\frac{\partial \Omega_U}{\partial \mu}, \quad (3)$$

$$\langle s^z \rangle = -\frac{\partial \Omega_U}{\partial h}. \quad (4)$$

Analytical expressions derived for the averages $\langle N \rangle$ and $\langle s^z \rangle$ are analyzed numerically in a wide range of U , h , μ and T parameters. The charge and spin degrees respond to an applied magnetic field (h) as well as electron or hole doping levels (i.e. chemical potential μ) and display clearly identifiable, prominent peaks, paving the way for rigorous definitions of Mott-Hubbard (MH), antiferromagnetic (AF), spin pseudogaps and related crossover behavior [13]. The exact expressions for charge susceptibility, $\chi_c = \frac{\partial \langle N \rangle}{\partial \mu}$ and spin susceptibility, $\chi_s = \frac{\partial \langle s^z \rangle}{\partial h}$ can be found as a function of U , h , μ and T from,

$$\langle X^2 \rangle - \langle X \rangle^2 = T \frac{\partial \langle X \rangle}{\partial x}, \quad (5)$$

where X corresponds to N or s^z and x to μ or h . Using maxima and minima in spin and charge susceptibilities, phase diagrams in a T vs μ plane for any U and h can be constructed. This approach also allows us to obtain QCP and rigorous criteria for various transitions, such as the MH crossover at half-filling and MH like bifurcations, using the evolution of peaks in charge or spin susceptibility [13] (see below).

B. Charge (pseudo) gap

We define canonical energies μ_{\pm} ,

$$\mu_+ = E(M+1, M'; U : T) - E(M, M'; U, T) \quad (6)$$

$$\mu_- = E(M, M'; U : T) - E(M-1, M'; U : T) \quad (7)$$

where $E(M, M'; U : T)$ is the canonical (ensemble) energy with a given number of electrons $N = M + M'$ determined by the number of up (M) and down (M') spins. At zero temperature the expressions (6) and (7) are identical to those introduced in [20]. At finite temperature, the calculated charge susceptibility is a differentiable function of N and μ . The peaks (i.e. maxima) in $\chi_c(\mu)$, which may exist in a limited range of temperature, are identified easily from the conditions, $\chi_c'(\mu_{\pm}) = 0$ with $\chi_c''(\mu_{\pm}) < 0$. We define $T_c(\mu)$ to be the temperature at which a (possible) peak is found in $\chi_c(\mu)$ at a given μ .

The positive charge gap for electron-hole (excito) excitations, $\Delta^{e-h}(T) > 0$, is defined by

$$\Delta^{e-h}(T) = \begin{cases} \mu_+ - \mu_- & \text{if } \mu_+ > \mu_- \\ 0 & \text{otherwise,} \end{cases} \quad (8)$$

as the separation between μ_+ and μ_- . The electron-hole instability $\Delta^{e-h}(T) > 0$ can exist in a limited range of temperatures and $U > U_c(T)$, with $\Delta^{e-h}(T) \equiv 0$ at $U \leq U_c(T)$. (In general, the critical parameter $U_c(T)$, identified and discussed in Sections III A and III B, depends also on h .) The energy gap, $\Delta^{e-h}(T) \geq 0$, serves as a natural order parameter in a multidimensional parameter space h, U, T and at $T \neq 0$ will be called a *pseudogap*, since χ has a small, but nonzero weight inside the gap. At $T = 0$, this gap $\Delta_0^{e-h} \equiv \Delta^{e-h}(0)$ will be labeled a *true gap* since χ_c is exactly zero inside.

The difference $\mu_+ - \mu_-$ is somewhat similar to the difference $I - A$ for a cluster, where I is the ionization potential and A the electron affinity. For a single isolated atom at half-filling and $T = 0$, $I - A$ is equal to U and hence the above difference represents a screened U , reminiscent of Herring's definition of U in transition elements [21].

C. Mott-Hubbard crossover

The thermodynamic quantities with fixed N (*canonical approach*) are certainly smooth, analytical functions of T and U . Thus, one may naively think that at half-filling and large U , there is no real cooperative phenomena at $T \sim U$ for transition from localized to delocalized electrons or at $T \sim \frac{t^2}{U}$ for transition from antiferromagnetic to paramagnetic state. At finite temperature, the thermodynamic quantities Ω_U and $\langle N \rangle$ are both analytic and smooth functions of T and μ . Although the charge susceptibility χ_c is also a differentiable function of μ and T at all $T > 0$, χ_c vs μ exhibits a weak, fourth order singularity at some critical temperature T_{MH} (*saddle point*) [13]. Thus the MH crossover at half-filling ($\mu = U/2$) can be

defined simply as a critical temperature T_{MH} , at which two peaks merge into one with $\mu = \mu_+ = \mu_- = U/2$ and $\chi'_c(\mu) = 0$ and $\chi''_c(\mu) = 0$, i.e. as the temperature corresponding to a point of inflexion in $\chi_c(\mu)$ [13]. This procedure gives a rigorous definition for the MH crossover temperature T_{MH} (from a localized into an itinerant state), at which the electron-hole pseudogap melts, i.e. $\Delta^{e-h}(T_{MH}) = 0$. The MH crossover, due to its many-body nature, is also a cooperative effect which may occur even for a single atom.

D. Spin (pseudo) gap

Analogously, we define a (positive) spin pairing gap between various spin configurations (projections of spin s) for a given number of electrons ($N = M + M'$) in the absence of a magnetic field ($h = 0$) as,

$$\Delta^s(T) = E(M + 1, M' - 1; U : T) - E(M, M'; U : T). \quad (9)$$

This corresponds to the energy necessary to make an excitation by overturning a single spin. Possible peaks in the zero magnetic field spin susceptibility $\chi_s(\mu)$, when monitored as a function of μ , can also be used to define an associated temperature, $T_s(\mu)$, as the temperature at which such a peak exists and the spin pseudogap as the separation (distance) between two such peaks.

E. AF (pseudo) gap and onset of magnetization

Similar to the (charge) plateaus seen in $\langle N \rangle$ vs μ , we can trace the variation of magnetization $\langle s^z \rangle$ vs an applied magnetic field h and identify the spin plateau features, which can be associated with staggered magnetization or short range antiferromagnetism. We calculate the critical magnetic field $h_{c\pm}$ for the onset of magnetization ($s^z \rightarrow \pm 0$), which depends on N and μ , by flipping a down spin, $h_{c+} = E(M + 1, M' - 1; U : T) - E(M, M'; U : T)$ or an up spin, $h_{c-} = E(M, M'; U : T) - E(M - 1, M' + 1; U : T)$ [22]. The spin singlet binding energy $\Delta^{AF}(T) > 0$ can be defined as,

$$\Delta^{AF}(T) = \frac{h_{c+} - h_{c-}}{2}, \quad (10)$$

and serves as a natural antiferromagnetic order parameter in a multidimensional parameter space U, T, μ . This will be called an *AF pseudogap* at nonzero temperature. We define T_{AF} as the temperature at which the pseudogap, $\Delta^{AF}(T) = 0$, vanishes and above which a paramagnetic state is found. An exact analytical expression for the AF spin gap in the ground state ($\Delta^{AF}(0)$) at half-filling was obtained in Ref. [13]. In what follows, all of the temperatures defined above, $T_c(\mu)$, $T_s(\mu)$ and $T_{AF}(\mu)$, will be used when constructing phase diagrams.

F. Pairing instability

To determine whether the cluster can support electron pairing at finite temperature despite the purely repulsive electronic interactions, the electron-electron (or hole-hole) pair binding energy,

$$\begin{aligned} \Delta^P(T) = & \\ [E(M - 1, M'; U : T) - E(M + 1, M'; U : T)] - & \\ 2[E(M, M'; U : T) - E(M + 1, M'; U : T)], & \quad (11) \end{aligned}$$

is calculated by adding or subtracting one electron near $N = M + M'$. The average energy $E(M, M'; U : T)$ is given for configurations with a fixed number of electrons N and spin magnetization $s^z = 0$ using our grand canonical ensemble approach. At zero temperature, the binding energy (11) is identical to the one introduced in Ref. [23].

Using the definitions for μ_{\pm} from Eqs. 6 and 7, electron-electron (or hole-hole) pair energy can also be written as,

$$\Delta^P(T) = \begin{cases} \mu_- - \mu_+ & \text{if } \mu_- > \mu_+ \\ 0 & \text{otherwise.} \end{cases} \quad (12)$$

In the ground state, the electron-pair binding energy gap at $\langle N \rangle \approx 3$ is fully developed at $U \leq U_c(T)$ when $\Delta^P(0) > 0$, i.e. $\mu_- > \mu_+$, which leads to the phase separation into $\langle N \rangle = 2$ and $\langle N \rangle = 4$ clusters (see Section III C) and an effective attraction between the electrons in $\langle N \rangle = 2$ cluster configuration [24]. *On the other hand, when $\mu_+ > \mu_-$, the condition $\Delta^{e-h}(T) > 0$ with $U > U_c(T)$ provides an electron-hole pairing mechanism as a precursor to antiferromagnetism [13].* We can define T_P as the temperature at which the pseudogap, $\Delta^P(T_P) = 0$, vanishes. The existence of particle-particle ($\Delta^P(T) > 0$) or particle-hole ($\Delta^{e-h}(T) > 0$) instability and the corresponding solution for a positive pseudogap ($\Delta(T) > 0$) can be formulated at an arbitrary $U > 0$ by combining both equations (8) and (12) in one as,

$$\Delta(T) = \begin{cases} \Delta^{e-h}(T) & \text{if } U > U_c(T) \\ \Delta^P(T) & \text{if } U < U_c(T). \end{cases} \quad (13)$$

At zero temperature, $\Delta(0) = 0$ at $U = 0$ or $U = U_c(0)$.

III. RESULTS

A. $\langle N \rangle$ and $\langle s^z \rangle$ vs μ and pseudogaps

In Fig. 2, we explicitly illustrate the variation of $\langle N \rangle \leq 4$ vs μ for various U values in order to track the variation of charge gaps with U . The opening of such gaps is a local correlation effect and clearly does not follow from long range order, as exemplified here. The true gaps at $\langle N \rangle = 1$ and $\langle N \rangle = 4$ develop for infinitesimal $U > 0$

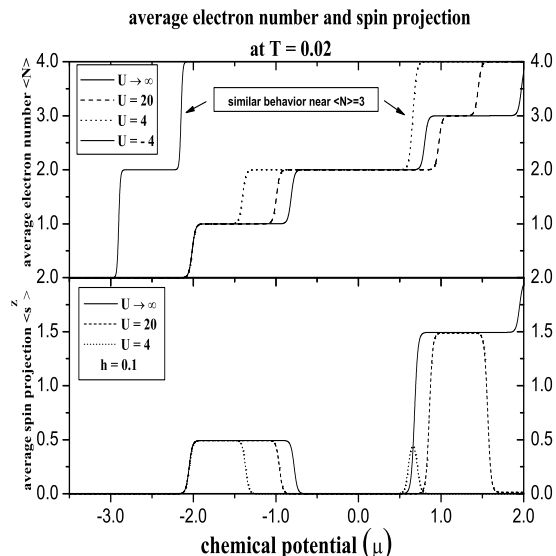


FIG. 2: Variation of average electron concentration $\langle N \rangle$ (top) and average spin $\langle s^z \rangle$ (bottom) vs μ for various U values at temperature $T = 0.02$. The vanishing of the charge gap near $\langle N \rangle = 3$ for $U = 4$ has implications related to pairing as discussed in the text. Note also that the spin plot has been obtained with an applied magnetic field of $h = 0.1$ and shows the stabilization of a magnetic state near $\langle N \rangle = 3$ for $U = 4$. At zero field, $\langle s^z \rangle = 0$ everywhere due to degeneracy between spin up and down states.

and increase monotonically. In contrast, the charge gap at $\langle N \rangle = 3$ opens at finite $U > U_c(T)$ (see Fig. 2). Thus at low temperature, $\langle N \rangle$ (expressed as a function of μ in Fig. 2) evolves smoothly for $U \leq U_c(T)$, showing finite leaps across the MH plateaus only at $\langle N \rangle = 1$, $\langle N \rangle = 2$. Such a density profile of $\langle N \rangle$ vs μ near $\langle N \rangle = 3$ closely resembles the one calculated in Fig. 2 for the attractive 4-site Hubbard cluster with $U = -4$ at $T = 0.02$ and is indicative of a possible particle pairing instability. At larger $U > U_c(T)$, an electron-hole gap is opened at $\langle N \rangle = 3$. Therefore the cluster at $U > U_c(0)$ behaves as a MH like insulator at all (allowed) integer numbers ($1 \leq N \leq 8$) with electron charge localized (non-Fermi liquid). In contrast, at $U \leq U_c(0)$ the chemical potential gets pinned upon doping in the midgap states at $\langle N \rangle \simeq 3$.

While Fig. 2 shows the magnetization at a relatively high magnetic field, its behavior at very low temperature, $T \rightarrow 0$ and infinitesimal magnetic field, $h \rightarrow 0$ is also noteworthy. In this case, as U increases, $\langle N \rangle$ and $\langle s^z \rangle$ vs μ near $\langle N \rangle = 3$ reveal islands of stability, due to phase separation (see Section III C), for various charge ($N = 2$ and $N = 4$) and spin (s and s^z) configurations as follows. Phase A ($U \leq U_c(0)$): particle-particle $\Delta^P(0) > 0$ and spin-spin $\Delta^{s^z=0}(0) > 0$ pair-

ing gaps with the minimal projection of spin $\langle s^z \rangle = 0$. Phase B ($U_c(0) < U < 4(2 + \sqrt{7}) \simeq 18.583$): particle-hole $\Delta^{e-h}(0) > 0$ and spin-spin $\Delta^{s^z=1/2}(0) > 0$ pairings with the spin $s = 1/2$ and unsaturated ferromagnetism, $\langle s^z \rangle = 1/2$ (triplet pairing) [22]. Phase C (large $U > 4(2 + \sqrt{7})$): particle-hole $\Delta^{e-h}(0) > 0$ pairing without spin gap ($\Delta^{s^z=3/2}(0) \equiv 0$) and maximum projection $\langle s^z \rangle = 3/2$ (saturated ferromagnetism) [25].

In Phase A for $U = 4$, charge and spin are coupled (i.e. no charge-spin separation), while in Phase B at $U = 6$, the charge and spin are partially decoupled (partial charge-spin separation). In Phase C for $U \rightarrow \infty$, the charge and spin are fully decoupled, when the charge gap saturates to its maximum value, $\rightarrow 2(2 - \sqrt{2})$, while the spin gap from $\langle s^z \rangle = 1/2$ to $\langle s^z \rangle = 3/2$, defined earlier in (9), vanishes (full charge-spin separation). Phase A, due to strong particle-particle coupling with double electron charge ($Q = 2e$) and zero spin ($s^z = 0$) with a majority of $\langle N \rangle = 2$ clusters, becomes a good candidate for the full 'bosonization' of charge and spin degrees of freedom and possible 'superconductivity'. In contrast, at even numbers of electrons, such as $\langle N \rangle \simeq 2$ in Fig. 2, there are electron-hole $\Delta^{e-h}(0) > 0$ and spin-spin $\Delta^{s^z=0}(0) > 0$ pairings at all U values, and therefore the charge $Q = 2e$ and spin $s^z = 0$ are both coupled and there is full charge-spin reconciliation, when the singlet-triplet spin excitation gap at quarter filling approaches the charge gap, $\Delta^{s^z=0} \equiv \Delta^{e-h} = 2(2\sqrt{2} - 1)$, as $U \rightarrow \infty$. Exactly at half filling, $\langle N \rangle = 4$, there is partial charge-spin separation at all finite $U > U_c(0)$. However, as $U \rightarrow \infty$ the charge MH gap $\Delta^{e-h}(0) \rightarrow \infty$ and the AF gap $\Delta^{s^z=0}(0) \rightarrow 0$ (vanishes); there is full charge-spin separation with saturated spin $\langle s^z \rangle = 2$ in this limiting case. Also, we find that for all U , the clusters with a single electron at $\langle N \rangle = 1$ is a MH like insulator: charge gap $\Delta^{e-h}(0) \rightarrow \infty$, while the spin gap $\Delta^{s^z=1/2}(0) \rightarrow 0$ with saturated spin $\langle s^z \rangle = 1/2$. For any given N in the charge sector, one can easily identify an insulator or a metallic liquid if $\Delta^{e-h}(0) > 0$ or $\Delta^{e-h}(0) \equiv 0$ respectively. Accordingly, it is also useful to distinguish a spin insulator, $\Delta^s(0) > 0$, or a spin liquid ($\Delta^s(0) \equiv 0$) state in the spin sector.

In Fig. 3, we show the evolution of charge susceptibility χ_c as a function of μ , which exhibits clearly identifiable sharp peaks. At low temperature, peak structures in $\chi_c(\mu)$ and zero magnetic field spin susceptibility, $\chi_s(\mu)$, are observed to develop in these clusters; between two consecutive peaks, there exists a pseudogap in charge or spin degrees. The opening of such distinct and separated pseudogap regions for spin and charge degrees of freedom (at low temperature) is a signature of corresponding charge and spin separation away from half-filling.

B. Pairing gap at $\langle N \rangle = 3$

At relatively large $U \geq U_c(T)$, the energy gap $\Delta_3^c(U : T) = E(4; U : T) + E(2; U : T) - 2E(3; U : T)$ becomes positive for $\langle N \rangle = 3$ (see Fig. 4). Its zero temperature

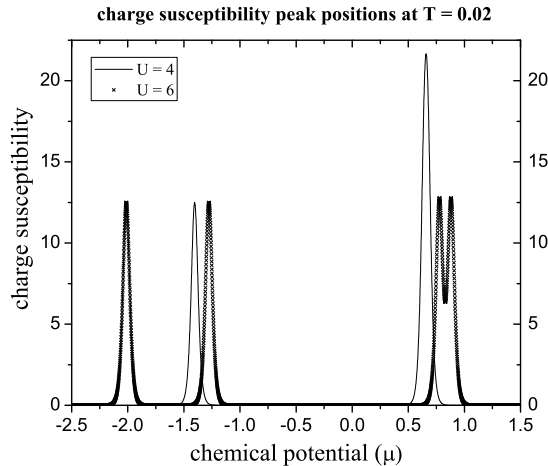


FIG. 3: The charge susceptibility *vs* chemical potential μ at $T = 0.02$ for two different U values ($U = 4$ and $U = 6$) below half-filling. Note that there are clearly identifiable peaks, and such peak positions, when monitored as a function of temperature, have been used to construct phase diagrams (see text).

value was first derived analytically [13] as,

$$\Delta_3^c(U : T = 0) = -\frac{2}{\sqrt{3}}\sqrt{(16t^2 + U^2)}\cos\frac{\gamma}{3} + \frac{U}{3} - \frac{2}{3}\sqrt{(48t^2 + U^2)}\cos\frac{\alpha}{3} + \sqrt{32t^2 + U^2 + 4\sqrt{64t^4 + 3t^2U^2}}, \quad (14)$$

where $\alpha = \arccos\left\{\left(\frac{4Ut^2}{3} - \frac{U^3}{27}\right)/\left(\frac{16t^2}{3} + \frac{U^2}{9}\right)^{\frac{3}{2}}\right\}$ and $\gamma = \arccos\left\{\left(4Ut^2\right)/\left(\frac{16t^2}{3} + \frac{U^2}{9}\right)^{\frac{3}{2}}\right\}$. Due to (ground state) level crossings [25], the exact expression (14) is valid only in a limited range of $U \leq 4(2 + \sqrt{7})$. The critical value, $U_c(0) = 4.58399938$, at which $\Delta_3^c(U_c : T = 0) = 0$, reported in Ref. [13], serves as an estimation of the accuracy of the gap value, which is slightly different from a value obtained in Ref. [18].

When $\Delta_3^c(U : T) = E(4; U : T) + E(2; U : T) - 2E(3; U : T)$ becomes negative for $U \leq U_c(T)$ as shown in Fig. 4, the $\langle N \rangle = 3$ states become less (energetically) favorable when compared with $\langle N \rangle = 2$ and $\langle N \rangle = 4$ states. This is a manifestation of electron binding where, despite bare electron repulsion, electron pairs experience an attraction [18, 23, 24]. We have also observed a similar vanishing of charge gaps for negative U values (see Fig. 2), where there is an inherent electron-electron attraction, supporting the above statement. For $U \geq U_c(T)$, the gap in the electron-hole channel is positive (i.e. $\Delta_3^c(T) > 0$) which favors excitonic, electron-hole pairing, similar to MH gap at half-filling.

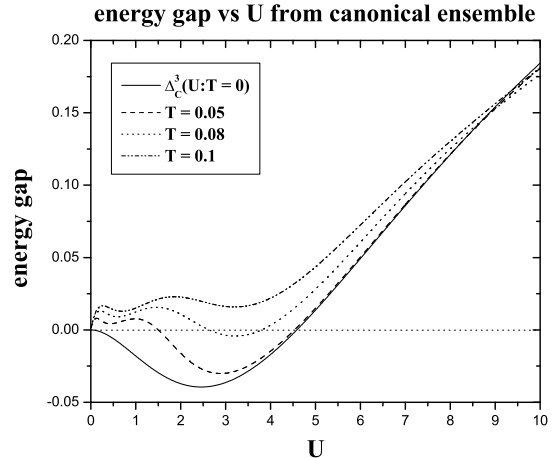


FIG. 4: The energy gap given by Eq. (14) at zero temperature and its evolution at several nonzero temperatures as a function of U obtained from the canonical ensemble. This is directly related to the electron-electron pairing gap ($U < U_c(T)$) and electron-hole charge gap ($U > U_c(T)$) as defined in the text. Note that charge pairing is unlikely to occur above temperature $T=0.08$. As previously, all energies are measured in units of t , the hopping parameter.

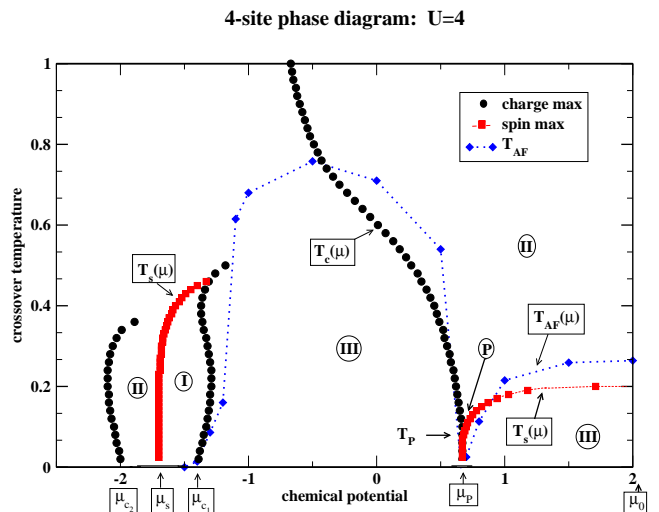


FIG. 5: Temperature T vs chemical potential μ phase diagram for the four-site cluster at $U = 4$ and $h = 0$, below half filling ($\mu \leq \mu_0$). Regions I and II are paramagnetic phases and quite similar to the ones found in the two-site cluster (Ref. [13]), showing strong charge-spin separation. Phase III is a MH antiferromagnetic phase (with zero spin). However, note the (new) line phase (labeled P) which consists of charge and spin fluctuations. This is a new feature seen in the 4-site cluster which suggests the existence of electron-electron pairing and phase separation into hole-poor and hole-rich regions at low temperature. For $U = 4$, pairing occurs below the temperature, $T_P=0.076$.

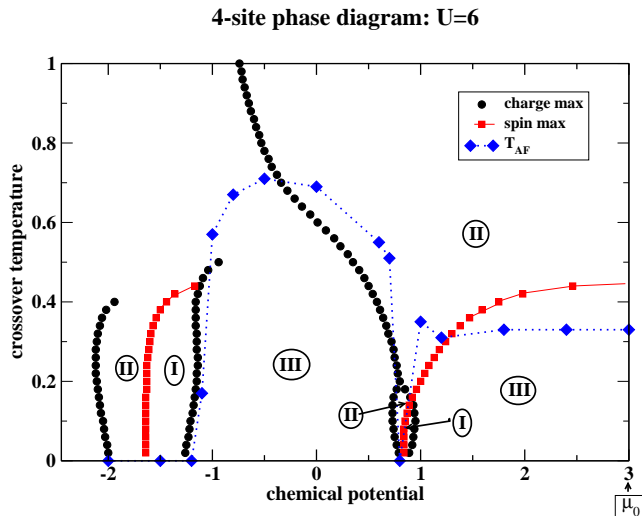


FIG. 6: Temperature T vs chemical potential μ phase diagram for the four site cluster at $U = 6$ and $h = 0$, below half-filling ($\mu \leq \mu_0$). Regions I, II and III are quite similar to the ones found for $U=4$ in Fig. 5, again showing strong charge-spin separation. However, a charge gap opens as a new bifurcation (I and II phases) which consists of charge and spin pseudogaps, (replacing the equilibrium line phase P in the previous figure, i.e. no electron-electron pairing here: see text for details). Temperature labels similar to those shown in Fig. 5 may be used here but have been suppressed for clarity.

C. Phase separation

It appears that the canonical approach yields an adequate estimation of a possible pair binding instability in the ensemble of small clusters at relatively low temperature. The competition between attraction and repulsion under hole-doping can lead to a ‘microscopic phase separation’, which comprises of an inhomogeneous structure of competing and coexisting hole-rich $\langle N \rangle = 2$ (hole-hole or electron-electron pairing), hole-poor $\langle N \rangle = 4$ (AF at half filling) and magnetic $\langle N \rangle = 3$ clusters. From Eqs. (6) and (7), it is apparent that the condition $\mu_- = \mu_+$ at $U = U_c(0)$ and $\langle N \rangle = 3$ defines a lower bound for the existence of a phase separation boundary that distinguishes a charge-spin separated region from a charge-spin coupled one.

If we neglect every second hopping term in the two dimensional square lattice, the system can be thought of as an ensemble of decoupled 4-site non-interacting clusters [16, 18], as shown in Fig. 1. New and important features appear if the number of electrons $\langle N \rangle = 3$ and total magnetization $\langle s^z \rangle = 0$ are kept fixed for the whole system of decoupled clusters, placed in the (particle) bath, by allowing the particle number on each separate cluster to fluctuate. One is tempted to think that due to symmetry, there is only a single hole on each cluster within the $\langle N \rangle = 3$ in ensemble. However, this statement reflects a simple average only. Due to thermal and quantum fluc-

tuations in the density of holes between the clusters (for $U < U_c(T)$), it is energetically more favorable to form pairs of holes. In this case, snapshots of the system at relatively low temperatures and at a critical value (μ_P in Fig. 5) of the chemical potential would reveal equal probabilities of finding (only) clusters that are either hole-rich $\langle N \rangle = 2$ or hole-poor $\langle N \rangle = 4$.

However, at higher temperatures when pairing coexists with magnetic spin fluctuations, there exists a small window of parameters which brings some stability to $\langle N \rangle = 3$ clusters above T_P . Thus the crossover from full separation (segregation) to the coexisting magnetic ($\langle N \rangle = 3$) and hole-rich ($\langle N \rangle = 2$) phases develops smoothly and depends on the degree of disorder, i.e. temperature. In section III A, it was shown how the changes in the parameter U affect the spin (magnetization) by changing the cluster configuration.

Phase separation of magnetic ($\langle N \rangle = 3$) and paired ($\langle N \rangle = 2$) states can also be triggered by increasing the magnetic field. The phase separation (i.e. segregation) into separate magnetic $\langle N \rangle = 3$ and hole-rich $\langle N \rangle = 2$ regions seen here at $\mu_- > \mu_+$, closely resembles the phase separation effect detected recently in super-oxygenated $\text{La}_{2-x}\text{Sr}_x\text{CuO}_{4+y}$, with various Sr contents [11]. Thus our results are consistent with the experimental observation that a small (applied) magnetic field mimics doping and promotes stability of the magnetic phase $\langle N \rangle = 3$ over the superconducting state $\langle N \rangle = 2$ near optimal doping.

In addition, our calculated probabilities (from the grand canonical ensemble) at low temperature show that, in the interval $\mu_+ < \mu < \mu_P$, $\langle N \rangle = 2$ clusters become the majority; i.e. we observe both, pairing and phase separation at low temperature. Note that phase separation here has a different origin and occurs at relatively weak coupling $U < U_c$ far from the level crossing regime, at which the spin gap vanishes. Therefore, the mechanism of phase separation here is different from the one found in Refs. [26, 27] at large U limit due to the *spin* density fluctuations ($h_+ < h_-$) and *spin* saturation. Indeed, the four-site cluster at large $U > 4(2 + \sqrt{7})$ reveals ferromagnetism in accordance with the Nagaoka theorem [25].

D. Phase diagrams

In Figs. 5 and 6, phase diagrams for the 4-site cluster ($U = 4$ and $U = 6$) are shown (see also Ref [28]). These have been constructed almost exclusively using the temperatures, $T_c(\mu)$, $T_s(\mu)$ and $T_{AF}(\mu)$, defined previously. We have identified the following phases in these diagrams: (I) and (II) are MH like paramagnetic phases with a charge pseudogap separated by a phase boundary where the spin susceptibility reaches a maximum, with $\Delta^{e-h}(T) > 0$, $\Delta^{AF} \equiv 0$; at finite temperature, phase I has a higher $\langle N \rangle$ compared to phase II; Phase (III) is a MH like antiferromagnetic insulator with bound charge and spin, when $\Delta^{e-h}(T) > 0$, $\Delta^s(T) > 0$, $\Delta^{AF}(T) > 0$;

(P) is a line phase for $U = 4$ with a vanished charge gap at $\langle N \rangle = 3$, now corresponding to the opening of a pairing gap ($\Delta^P(T) > 0$) in the electron-electron channel with $\Delta_3^c(U : T) < 0$. We have also verified the well known fact that the low temperature behavior in the vicinity of half-filling, with charge and spin pseudogap phases coexisting, represents an AF insulator [13]. However, away from half-filling, we find very intriguing behavior in thermodynamical charge and spin degrees of freedom.

In both phase diagrams, we find similar paramagnetic MH (I), (II) charge-spin separated phases in addition to the AF (III) phase where spin and charge are bounded. In Fig. 6, spin-charge separation in phases (I) and (II) originates for relatively large $U (= 6)$ in the underdoped regime. In contrast, Fig. 5 shows the existence (at $U = 4$) of a line phase (with pairing) similar to $U < 0$ case with electron pairing ($\Delta^P(T) > 0$), when the chemical potential is pinned up on doping within the highly degenerate midgap states near (underdoped) $1/8$ filling.

E. Quantum critical points

Among other interesting results, rich in variety, sharp transitions at QCP near $\langle N \rangle = 3$ are found in the ground state at $U > U_c(0)$ between phases with true charge and spin gaps; for infinitesimal $T \rightarrow 0$, these gaps are transformed into ‘pseudogaps’ with some nonzero weight between peaks (or maxima) in susceptibilities monitored as a function of doping (i.e. μ) as well as h . In the limiting case $T_c(\mu_c) \rightarrow 0$, the QCP doping, μ_c , defines a sharp MH like (AF) like transition with diverging χ_c [13]. At the QCP doping, μ_s , with $T_s(\mu_s) \rightarrow 0$, the zero spin susceptibility, χ_s , also exhibits a maximum.

In Fig. 6, the critical temperature $T_s(\mu)$ falls abruptly to zero at the QCP doping, μ_s (true only for $U > U_c(0)$), implying [8] that the (spin) pseudogap can exist independently of possible particle pairing in Fig. 6. In contrast, for $U < U_c(0)$ and low temperature, there is no charge-spin separation near $\langle N \rangle = 3$. Therefore in Fig. 5 at $U = 4$ ($U < U_c(0)$) we do not observe any QCP associated with μ_s or μ_c close to $\langle N \rangle = 3$. Instead, Fig. 5 shows the existence of a line phase (with pairing) similar to the attractive $U < 0$ case with a spin pseudogap, which exists only at finite temperature $T_s(\mu) > 0$, and electron pairing ($T_P > T_s$), when the chemical potential is pinned up on doping within the highly degenerate midgap states near (underdoped) $1/8$ filling.

We have also seen that a reasonably strong magnetic field can bring about phase separation and has a dramatic effect (mainly) on the QCP at μ_s , at which the spin pseudogap disappears. It is evident from our exact results that presence of QCP at zero temperature and critical crossovers at $T_c(\mu)$, $T_s(\mu)$ and $T_{AF}(\mu)$ temperatures, gives strong support for the cooperative character of existing phase transitions and crossovers similar to those seen in large thermodynamic systems at finite temperatures [29, 30].

F. Charge-spin separation

Charge-spin separation effect is fundamental for understanding of the generic features common for small and large thermodynamic systems. We formulated exact criteria when the charge and spin excitations are decoupled at $U > U_c(T)$. There is controversy regarding the nature of MH and AF transitions and relation between their consequent critical temperatures [13]. In Figs. 5 and 6, the charge, decoupled from spin degree of freedom, condenses at temperatures below T_c while AF spin correlations near half-filling are seen to develop at lower temperatures $T_{AF}(\mu) < T_c(\mu)$ [13]. However, in the limited range close to $\mu \geq \mu_c$, there is a reverse behavior, $T_{AF}(\mu) \geq T_c(\mu)$. Electrons were until recently thought to carry their charge and spin degrees of freedom equally; however accurate studies of thermodynamic response functions in nanoscale clusters show that in real materials, these two degrees of freedom are relatively independent from one another and can condensate at different doping levels μ_c , μ_s and transition temperatures $T_c(\mu)$, $T_{AF}(\mu)$ and $T_s(\mu)$ shown in Fig. 5 and Fig. 6.

The charge-spin separation is an unusual behavior of electrons in some materials under certain conditions permitting the formation of two independent (bound) electron-electron or electron-hole pairs (quasiparticles) in charge sectors and spin singlet and triplet states in spin sectors. The spin quasiparticle only carries the spin degree of the electron but not the charge, while the charge quasiparticle has spin equal to zero but its electric charge equals either zero (electron-hole pair) or a charge of two electrons (electron-electron pair). We find that at large $U > U_c(T)$, clusters with localized charge are favored over itinerant ones.

As an important footnote, in the noninteracting $U = 0$ case shown in Fig. 7, the charge and spin peaks follow one another (in sharp contrast to the $U = 4$ and 6 cases). In regions I and II, positions of charge (as well as spin) maxima and minima coincide indicating that there is no charge-spin separation, even in the presence of a magnetic field. In the entire range of μ , the charge and spin fluctuations directly follow one another without charge-spin separation. Our detailed analysis of the (responses such as) variation of electron concentration $\langle N \rangle$, zero magnetic field magnetization $\langle s^z \rangle$ vs μ and various fluctuations shows that there is no charge-spin separation and both, the spin and charge degrees, closely follow each other. Thus, at $U = 0$ the spin and charge degrees are strongly coupled to one another. On the other hand, the charge-spin separation effect at $U \neq 0$ led to rigorous definitions of Mott-Hubbard like, antiferromagnetic, spin pseudogaps, particle-particle pairings and related crossovers.

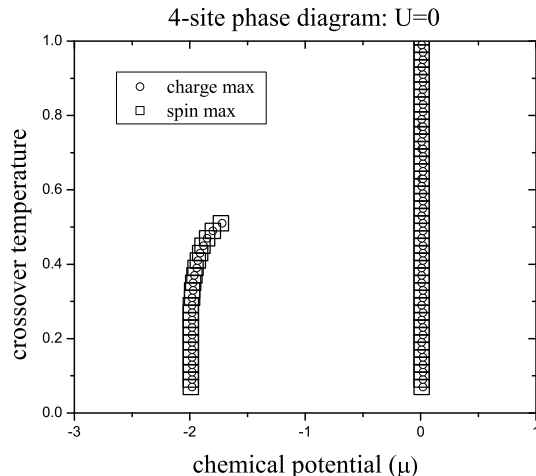


FIG. 7: The single particle or ‘noninteracting’ ($U = 0$) case, illustrating the positions of charge and spin susceptibility peaks in a $T - \mu$ space for the 4-site cluster at $\mu < 1$ (half-filling is at $\mu_0 = 0$). Note how the charge and spin peaks follow one another. Even in the presence of a nonzero magnetic field there is no charge-spin separation.

IV. CONCLUSION

In summary, we have illustrated how to obtain phase diagrams and identify the presence of temperature driven crossovers, quantum phase transitions and charge-spin separation for any $U \geq 0$ in the four-site Hubbard *nanocluster* as doping (or chemical potential) is varied. Specifically, our exact solution pointed out an important difference between the $U = 4$ ($U < U_c(0)$) and $U = 6$ ($U > U_c(0)$) phase diagrams at finite temperature in the vicinity of hole doping $\approx 1/8$ which can be tied to possible electron-electron pairing due to overscreening of the repulsive interaction between electrons in the former.

The resulting phase diagram with competing hole-rich ($\langle N \rangle = 2$), hole-poor ($\langle N \rangle = 4$) and magnetic ($\langle N \rangle = 3$) phases captures also the essential features of phase separation in doped $\text{La}_{2-x}\text{Sr}_x\text{CuO}_{4+y}$ [11]. Our analytical results near $\langle N \rangle \approx 3$ strongly suggest that particle pairing can exist at $U < U_c(T)$, while particle-hole binding is presumed to occur for $U > U_c(T)$. It is also clear that short-range correlations alone are sufficient for pseudogaps to form in small and large clusters, which can be linked to the generic features of phase diagrams in temperature and doping effects seen in the HTSCs. The exact cluster solution shows how charge and spin (pseudo) gaps are formed at the microscopic level and their behavior as a function of doping (i.e. chemical potential), magnetic field and temperature. The pseudogap formation can also be associated with the condensation of spin and charge degrees of freedom below spin and charge crossover temperatures. In addition, our exact analytical and numerical calculations provide important benchmarks for comparison with Monte Carlo, RSRG, DCA and other approximations.

Finally, our results on the existence of QCP and crossover temperatures show the *cooperative nature* of phase transition phenomena in finite-size clusters similar to large thermodynamic systems. The small *nanoclusters* exhibit a pairing mechanism in a limited range of U , μ and T and share very important intrinsic characteristics with the HTSCs apparently because in all these ‘bad’ metallic high T_c materials, local interactions play a key role. As charge and spin susceptibilities (5), energy fluctuations are related to the specific heats and these new results for the 4-site and larger clusters, which provide further support to our picture developed here, will be reported elsewhere.

One of us (ANK) thanks Steven Kivelson for interest and helpful discussion by communicating the results of their preprint (Ref. [18]). This research was supported in part by the U.S. Department of Energy under Contract No. DE-AC02-98CH10886.

-
- [1] P. W. Anderson, *Science* **235**, 1196 (1987).
 - [2] V. Emery and S. A. Kivelson, *Nature (London)*, **374**, 434 (1995).
 - [3] T. Timusk and B. Statt, *Rep. Prog. Phys.* **62**, 61 (1999).
 - [4] S. A. Kivelson *et al.*, *Rev. Mod. Phys.* **75**, 1201 (2003).
 - [5] D. S. Marshall *et al.*, *Phys. Rev. Lett.* **76**, 4841 (1996).
 - [6] Andrea Damascelli, Zahid Hussain, Zhi-Xun Shen, *Rev. Mod. Phys.* **75**, 473 (2003).
 - [7] P. W. Anderson, *Adv. Rev.* **46**, 3 (1997).
 - [8] G. V. M. Williams, J. L. Tallon and J. W. Loram, *Phys. Rev. B* **58**, 15053 (1998).
 - [9] V. J. Emery, S. A. Kivelson and O. Zachar, *Phys. Rev. B* **56** 6120 (1997).
 - [10] M. Matsuda, M. Fujita, K. Yamada, R. J. Birgeneau, Y. Endoh and G. Shirane, *Phys. Rev. B* **65**, 134515 (2002).
 - [11] H. E. Mohottala, B. O. Wells, J. I. Budnick, W. A. Hines, C. Niedermayer, L. Udby, C. Bernard, A. R. Moodenbaugh and Fang-Cheng Chou, *Nature (London)*, **5**, 377 (2006).
 - [12] Y. Zha, V. Barzykin and D. Pines, *Phys. Rev. B* **54**, 7561 (1996).
 - [13] A. N. Kocharian, G. W. Fernando, K. Palandage and J. W. Davenport, *J. Mag. Mag. Mater.*, **300**, e585-590 (2006).
 - [14] D. Sénéchal, D. Perez, and M. Pioro-Ladriere, *Phys. Rev. Lett.* **84**, 522 (2000).
 - [15] Jean-Paul Malrieu and Nathalie Guihery, *Phys. Rev. B* **63**, 085110 (2001).
 - [16] E. Altman and A. Auerbach, *Phys. Rev. B* **65**, 104508 (2002).

- [17] M. Jarrell, Th. Maier, M.H. Hettler, and A.N. Tahvil-darzadeh, *Europhys. Lett.* **56**, 563 (2001).
- [18] Wei-Feng Tsai and Steven A. Kivelson, *Inhomogeneous Hubbard Models: from Weak to Strong Coupling*, cond-mat/0601113 (2006); APS March Meeting Bulletin **51** (1), Part 2 (2006).
- [19] R. Schumann, *Ann. Phys.* **11**, 49 (2002).
- [20] E. H. Lieb, and F. Y. Wu, *Phys. Rev. Lett.* **20**, 1445 (1968).
- [21] C. Herring, "Exchange Interactions Among Itinerant Electrons", in *Magnetism Vol IV*, G.T. Rado and H. Suhl eds., Academic Press, New York, 1966.
- [22] A. N. Kocharian and Joel H. Sebold, *Phys. Rev.* **B53**, 12804 (1996).
- [23] J. E. Hirsch, S. Tang, E. Loh Jr., D. J. Scalapino, *Phys. Rev. Lett.* **60**, 1668 (1988); R. M. Fye, M. J. Martins, and R. T. Scalettar, *Phys. Rev.* **B42**, R6809 (1990).
- [24] Steven R. White, Sudip Chakravarty, Martin P. Gelfand, and Steven A. Kivelson, *Phys. Rev.* **B45**, 5062 (1992).
- [25] D. C. Mattis, *Int. J. Nanoscience* **2**, 165 (2003).
- [26] P. B. Visscher, *Phys. Rev. B* **10** 943 (1974).
- [27] V. J. Emery, S. A. Kivelson and H. Q. Lin *Phys. Rev. Lett.* **64** 475-478 (1990).
- [28] A. N. Kocharian, G. W. Fernando, K. Palandage and J. W. Davenport, *Phase Diagrams and Charge-Spin Separation in Two and Four Site Hubbard Clusters*, cond-mat/0510609 (2005).
- [29] W. Langer, M. Plischke, and D. M. Mattis, *Phys. Rev Lett.*, **23** 1448 (1969).
- [30] M. Cyrot, *Phys. Rev Lett.*, **25** 871 (1970).